Exchange bias effects in Fe nanoparticles embedded in an antiferromagnetic Cr2O3 matrix

Jordi Sort, V. Langlais, Stefania Doppiu, Bernard Dieny, Santiago Suriñach, J. S. Muñoz, M. D. Baró, Christophe Laurent, Josep Nogués

Exchange bias effects in Fe nanoparticles embedded in an antiferromagnetic Cr_2O_3 matrix

J Sort[1,2], V Langlais[2], S Doppiu[2], B Dieny[1], S Suriñach[2], J S Muñoz[2], M D Baró[2], Ch Laurent[3] and J Nogués[4]

[1] SPINTEC/CEA-Grenoble, 17 Avenue des Martyrs, 38054 Grenoble Cedex 9, France
[2] Departament de Física, Universitat Autònoma de Barcelona, 08193 Bellaterra, Barcelona, Spain
[3] Centre Interuniversitaire de Recherche et d'Ingénierie des Matériaux, Bâtiment 2R1, Université Paul-Sabatier, 31062 Toulouse Cedex 4, France
[4] Institució Catalana de Recerca i Estudis Avançats (ICREA) and Departament de Física, Universitat Autònoma de Barcelona, 08193 Bellaterra, Barcelona, Spain

Abstract

Powders consisting of ferromagnetic (FM) Fe nanoparticles, of about 7 nm in size, embedded in an antiferromagnetic (AFM) Cr_2O_3 matrix have been obtained by high-temperature reduction under a hydrogen atmosphere of a mixed Cr–Fe oxide. This FM–AFM system exhibits exchange bias effects, i.e. a loop shift (H_E) and coercivity enhancement (ΔH_C), when field-cooled through the Néel temperature, T_N, of Cr_2O_3. The exchange bias properties were measured as a function of temperature. H_E and ΔH_C are found to vanish at about $T_N(Cr_2O_3)$, indicating a good quality AFM matrix. Hence, high-temperature reduction of mixed oxides is demonstrated to be a suitable technique to develop new types of FM–AFM exchange-biased nanoparticles, from which novel applications of this phenomenon may be developed.

1. Introduction

Exchange bias is the shift of the hysteresis loop along the magnetic field axis direction, which originates as a result of exchange interactions between a ferromagnetic (FM) and an antiferromagnetic (AFM) material [1–4]. The loop shift is often accompanied by an enhancement of the coercivity. These phenomena were discovered about half a century ago in partially oxidized Co particles [5]. During the last decade, the bulk of the research in exchange bias has been mainly focused on thin film systems due to their applicability in spin valves for magnetic recording and sensor devices [6]. However, recently the study of exchange bias effects in fine-particle systems is recovering its importance, since it has been demonstrated that FM–AFM exchange interactions can be useful to enhance the hard magnetic properties of permanent magnets [7–9] or to beat the superparamagnetic limit in FM nanoparticles [10].

Nevertheless, soon after the discovery of exchange bias, it became clear that applications of exchange bias effects in fine-particle systems would be limited. This was mainly due to the fabrication process, which was based on chemical treatments of FM particles to obtain reacted AFM phases, creating core (FM)–shell (AFM) particles. As a result, the number of fine-particle systems in which exchange bias could be observed was rather restricted, since the AFM had to be obtained from a simple chemical reaction of the FM core. Thus, basically, only transition metal particles embedded in their AFM native oxides (e.g. Co–CoO [5], Ni–NiO [11] or Fe–Fe_3O_4 [12]), oxide nanoparticles with different oxidation states (e.g. CrO_2 (ferrimagnetic)–Cr_2O_3 (antiferromagnetic) [13]) or transition metal nanoparticles surrounded by chemically obtained sulfides or nitrides (e.g. Fe–FeS [14], Co–CoN [15], Fe–Fe_2N [16]), have been studied. This severely restricts the technological applications of these types of materials. For example, many of the systems exhibit blocking temperatures, T_B (i.e. the temperature at which the exchange bias effects vanish [1]), far below room temperature [5, 11–16]. Moreover, it is generally not possible to obtain AFM phases by chemically treating many FM materials, e.g. hard magnetic materials. Just recently, exchange bias effects have been induced in particles, by means of ball milling, in some combinations of FM and AFM phases *not* derived from the same transition

metal (e.g. Co–NiO, Co–FeS or $SmCo_5$–NiO) [7, 8]. However, the size of the resulting FM and AFM particles obtained by ball-milling is typically of the order of a few micrometres. Hence, new ultrafine particle synthesis methods are necessary to investigate exchange bias effects in FM–AFM mixtures consisting of particles of only a few nanometres in size. Indeed, there is an increasing interest in lithography-fabricated exchange-biased nanostructures [17–19], mainly due to the drastic increase of the areal density of recording media, which demands a miniaturization of the spin valve-based magnetic sensor devices. However, most lithography techniques cannot yet reliably produce nanostructures of a few nanometres [20].

In this paper, we present the synthesis of *nanometric* FM particles embedded in an AFM matrix, in which the FM and the AFM phases are derived from *different* transition metals. This is carried out by high temperature reduction under a hydrogen atmosphere of a mixed oxide (i.e. an oxide of two different transition metals). This process yields a selective reduction of one of the transition metals (the FM) leaving the other in the oxidized state (the AFM). The resulting material exhibits exchange bias when it is field-cooled from above the Néel temperature of the AFM.

2. Experimental details

Selective high temperature reduction under a hydrogen atmosphere of $Cr_{1.8}Fe_{0.2}O_3$ powders was used to produce a microstructure consisting of Fe nanoparticles embedded in an AFM Cr_2O_3 matrix [21]. A binary oxide solution was prepared by thermal decomposition and air calcination of mixed oxalate precursors. The calcinations, carried out at 1100 °C, allowed the crystallization of the solid solutions. Subsequently, the reduction of the solid solution was performed in pure dry hydrogen at 1200 °C for 2 h, giving rise to a Fe–Cr_2O_3 nanocomposite. Morphological and structural characterization was carried out by transmission electron microscopy (TEM) and x-ray diffraction (XRD).

To induce exchange bias, the as-prepared powders were cooled in the presence of a magnetic field of variable strength ($0 < H_{FC} < 50$ kOe) from room temperature to $T = 10$ K. Magnetic hysteresis loops were subsequently recorded at several temperatures when heating from 10 to 350 K by means of a vibrating sample magnetometer (VSM), applying a maximum field of 50 kOe, i.e. enough to ensure full saturation of the powders.

3. Results and discussion

Shown in figure 1 is a TEM micrograph of the as-prepared powders. It can be seen that the particles have rounded shapes and are about 200 nm in size. Each of them consists of a host of darker spots with sizes ∼7 nm, corresponding to metallic nanoparticles (high contrast) (Fe), which are embedded in an oxide matrix (low contrast) (Cr_2O_3). The Fe nanoparticles exhibit a log-normal distribution with a mean particle size of 7 nm and a standard deviation of $\sigma_{\log-\mathrm{norm}} = 2$ nm (figure 1(b)). The existence of the two-phase mixture (i.e. α-Fe and corundum-like Cr_2O_3) was confirmed by XRD. Using a full-pattern fitting procedure (i.e. Rietveld method) [22] the weight percentage of Fe was estimated to be around 10%, which is in qualitative agreement with the TEM observations.

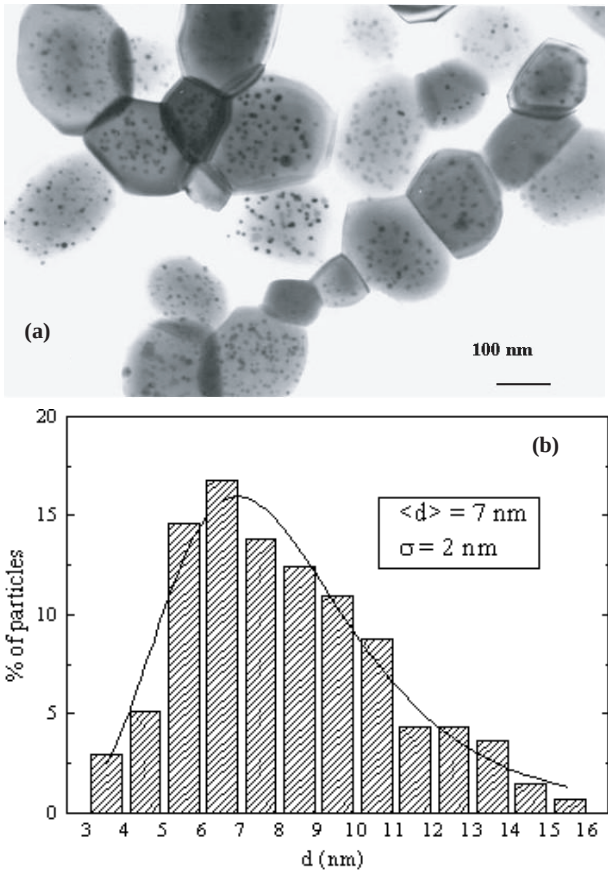

Figure 1. (a) TEM micrograph of Fe nanoparticles embedded in a Cr_2O_3 matrix; (b) Fe particle size distribution, as evaluated from the TEM image.

Moreover, the cell parameters of Fe ($a = 0.2872(1)$ nm) and Cr_2O_3 ($a = 0.4960(1)$ nm and $c = 0.1358(1)$ nm) were found to correspond to those tabulated for these two phases [23], indicating the absence of interdiffusion between them.

The temperature dependence of the exchange bias field, H_E, and coercivity, H_C, after field cooling ($H_{FC} = 50$ kOe) are shown in figures 2(a) and (b), respectively. As shown in figure 2(a), a small exchange bias, $H_E = 9$ Oe, is obtained at $T = 10$ K. The exchange energy per surface unit of the FM–AFM coupling can be estimated, in a first approximation, as $\sigma = (H_E M_S 4/3\pi r^3)/4\pi r^2 = H_E M_S r/3$, where M_S is the saturation magnetization of Fe at $T = 10$ K and r is the particle radius (assuming they are spherical). Taking $r = 4$ nm, one obtains $\sigma_{(T=10\ \mathrm{K})} = 3 \times 10^{-4}$ erg cm^{-2}, which is about one order of magnitude lower than the exchange energy, evaluated at room temperature, for FM–AFM thin films containing Cr_2O_3 as antiferromagnet and lower than the typical values of σ for the majority of FM–AFM thin film systems [1]. Note that a small exchange bias is somewhat expected from the low anisotropy of Cr_2O_3 [24], in agreement with measurements in systems containing Cr_2O_3, either in nanostructured [25] or in thin film form [26], although large loop shifts have been observed in CrO_2–Cr_2O_3 core–shell particles [13]. Moreover, the smaller value of σ for the Fe-Cr_2O_3 nanoparticles, when compared with FM–AFM thin films containing Cr_2O_3 as AFM, could be due to a less effective spin alignment that the Fe nanoparticles could induce on the neighbouring Cr_2O_3 spins during the field-

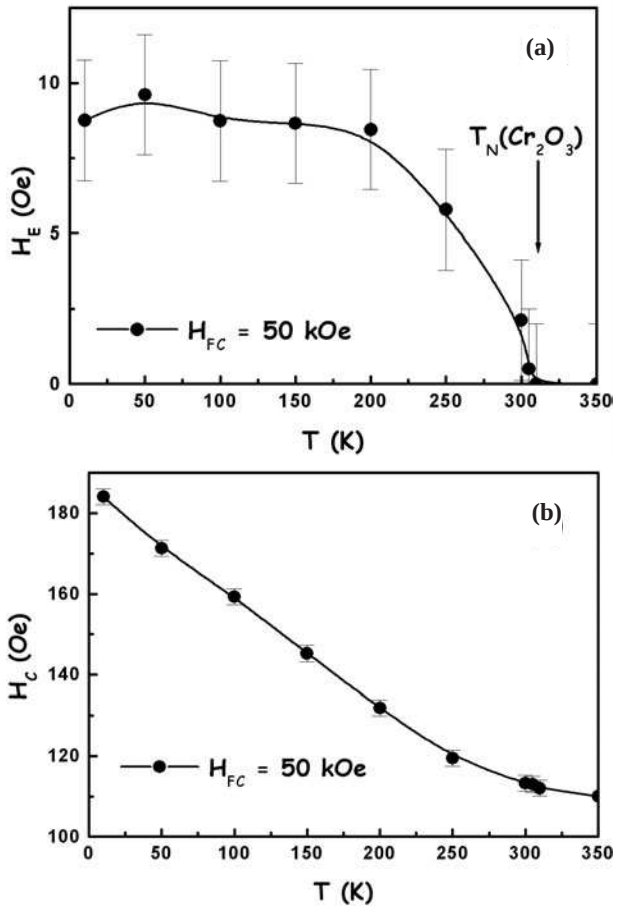

Figure 2. Temperature dependence of the exchange bias, H_E (in (a)), and coercivity, H_C (in (b)), after cooling from room temperature in a magnetic field $H_{FC} = 50$ kOe.

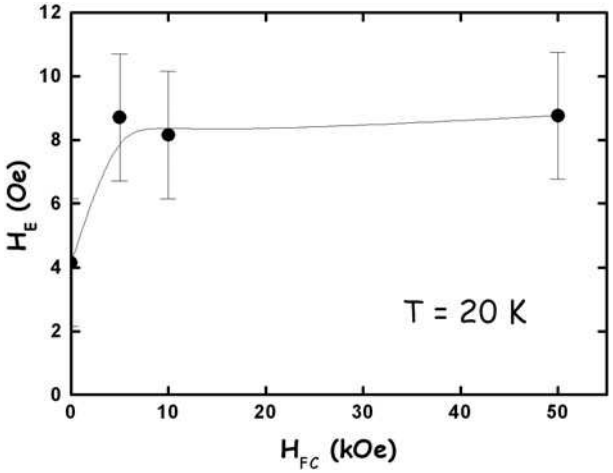

Figure 3. Dependence of the exchange bias, H_E, measured at $T = 20$ K, on the magnetic field applied during the cooling process from room temperature, H_{FC}.

cooling procedure and the concomitant more random character of FM–AFM interactions in the powder system compared to exchange-biased FM–AFM thin films. $H_E(T)$ has a rather constant value until the temperature approaches 200 K, where $H_E(T)$ starts to decrease, until it vanishes, due to the thermally induced loss of magnetic stability of the AFM, at a blocking temperature, T_B, of about $T_B \sim 307 \pm 5$ K. Thus, the fact that $T_B \approx T_N(Cr_2O_3) = 307$ K implies a high degree of crystallinity of the AFM phase [1], in contrast with earlier core–shell nanoparticles, in particular CrO_2–Cr_2O_3 core–shell nanoparticles [13], which show $T_B \ll T_N$. Remarkably, the temperature dependence of H_E resembles more those observed in epitaxial and high quality thin film systems (i.e. Brillouin-like $H_E(T)$) [27], rather than the ones in polycrystalline systems (usually more linear $H_E(T)$) [28]. This probably also indicates a high quality of the oxide matrix. Moreover, the absence of training effects [26] in this system (observed in CrO_2–Cr_2O_3 core–shell nanoparticles [13]) indicates once more a good quality Cr_2O_3 matrix [1].

As can be seen in figure 2(b), the system also exhibits a coercivity enhancement, ΔH_C, from $H_C = 112$ Oe at room temperature to $H_C = 185$ Oe at 10 K. Since an increase of coercivity could also be induced by the concomitant increase of the magnetocrystalline anisotropy of the FM nanoparticles at low temperatures, H_C was also measured after a zero-field-cooling (ZFC) procedure. As expected, H_C (ZFC) = 165 Oe is lower than the one obtained after field cooling, confirming the existence of AFM–FM exchange coupling. However, it is important to remember that exchange bias effects can also be present even after a ZFC procedure [29]. This is shown, in our case, by the presence of a small exchange bias, $H_E = 4$ Oe, even after ZFC, arising from the effect of the remanent moment of the Fe nanoparticles on the Cr_2O_3 matrix during the ZFC process.

H_C after field cooling decreases as the temperature is increased, leveling off at temperatures around $T_N(Cr_2O_3) \sim 310$ K. However, since the FM nanoparticles remain magnetic above $T_N(Cr_2O_3)$ the coercivity remains finite, $H_C \sim 100$ Oe.

It is noteworthy that, using the bulk anisotropy value for Fe (i.e. $K = 5 \times 10^5$ erg cm^{-3}), the expected superparamagnetic blocking temperature, T_B, for 7 nm Fe nanoparticles would be $T_B = (KV)/25k_B = 40$ K, where V is the particle volume and k_B is the Boltzmann constant. However, in our case, we observe that the Fe nanoparticles remain ferromagnetic at least up to $T = 350$ K. This can be due to surface effects or dipolar interactions, enhancing the apparent anisotropy of the nanoparticles [30, 31], although the exchange interactions between the FM nanoparticles and the AFM matrix could also be playing a role in stabilizing the magnetic moment against thermal fluctuations, particularly below $T_N(Cr_2O_3)$ [10].

Finally, since Cr_2O_3 has a rather low anisotropy (2×10^5 erg cm^{-3} [24]), the system could be prone to field-induced effects [32] (as observed CrO_2–Cr_2O_3 core–shell nanoparticles [13]), such as AFM spin-flop or AFM domain wall motion. Hence, exchange bias was studied as a function of the cooling field. As shown in figure 3, after the initial increase in H_E when going from $H_{FC} = 0$ Oe to 5 kOe, the loop shift remains fairly constant for larger cooling fields. This could indicate that, due to the random nature of the samples, the field-induced effects could be exceedingly small in this system. Alternatively, any field-induced effects may take place at fields above $H = 50$ kOe. For example, the spin-flop field in Cr_2O_3 is about $H_{SF} = 60$ kOe at low temperatures [33]. However, due to the small size of the oxide particles, the transition field is expected to be reduced [34]. Nevertheless, the degree of reduction may be insufficient to be observed with a 50 kOe

field. Note that the fact that some field effects were observed in CrO_2–Cr_2O_3 core–shell nanoparticles [13] may be due to the thin Cr_2O_3 shell and its small crystallite size, compared to the microstructure in our samples.

4. Conclusions

In summary, it has been shown that FM *nanoparticles* (α-Fe) embedded in an AFM matrix (Cr_2O_3), in which the FM and AFM phases are *not derived* from the same transition metal, can be obtained by means of selective high temperature reduction under a hydrogen atmosphere of mixed oxides. The resultant nanocomposite particles exhibit exchange bias effects (i.e. a shift of the hysteresis loop and an enhancement of coercivity) when they are field-cooled from above the blocking temperature of the system. As expected, both H_E and H_C are found to be reduced if the system is cooled in zero magnetic field. It is remarkable that, contrary to other processing techniques to create mixtures of FM and AFM powders, high temperature reduction seems to be an appealing method to produce very small FM particles (of just a few nanometres in size) embedded in an AFM matrix, a microstructure which is interesting in exploiting novel applications of the exchange bias phenomena.

Acknowledgments

Partial financial support from NEXBIAS (HPRN-CT 2002-00296), CICYT (MAT2001-2555), DGR (2001SGR00189), the Generalitat de Catalunya (ITT2000-14) and Midi Pyrénées Council (CTP Grant) is gratefully acknowledged. VL and JS thank the NEXBIAS European Research Training Network for its financial support.

References

[1] Nogués J and Schuller I K 1999 *J. Magn. Magn. Mater.* **192** 203
[2] Berkowitz A E and Takano K 1999 *J. Magn. Magn. Mater.* **200** 552
[3] Stamps R L 2000 *J. Phys. D: Appl. Phys.* **33** R247
[4] Kiwi M 2001 *J. Magn. Magn. Mater.* **234** 584
[5] Meiklejohn W H and Bean C P 1956 *Phys. Rev.* **102** 1413
[6] Dieny B, Speriosu V S, Parkin S S P, Gurney B A, Wilhoit D R and Mauri D 1991 *Phys. Rev.* B **43** 1297
[7] Sort J, Nogués J, Amils X, Suriñach S, Muñoz J S and Baró M D 1999 *Appl. Phys. Lett.* **75** 3177
[8] Sort J, Nogués J, Suriñach S, Muñoz J S, Baró M D, Chappel E, Dupont F and Chouteau G 2001 *Appl. Phys. Lett.* **79** 1142
Sort J, Suriñach S, Muñoz J S, Baró M D, Nogués J, Chouteau G, Skumryev V and Hadjipanayis G 2002 *Phys. Rev.* B **65** 174420
[9] Stoyanov S, Skumryev V, Zhang Y, Huang Y, Hadjipanayis G C and Nogués J 2003 *J. Appl. Phys.* **93** 7592
[10] Skumryev V, Stoyanov S, Zhang Y, Hadjipanayis G, Givord D and Nogués J 2003 *Nature* **423** 850
[11] Yao Y D, Chen Y Y, Tai M F, Wang D W and Lin H M 1996 *Mater. Sci. Eng.* A **217/218** 281
[12] Löffler J, van Swygenhoven H, Wagner W, Meier J, Doudin B and Ansermet J P 1997 *Nanostruct. Mater.* **9** 523
[13] Yu M H, Devi P S, Lewis L H, Oouma P, Parise J B and Gambino R J 2003 *Mater. Sci. Eng.* B **103** 262
[14] Greiner J H, Croll I M and Sulich M 1961 *J. Appl. Phys.* **32** 188S
[15] Lin H M, Hsu C M, Yao Y D, Chen Y Y, Kuan T T, Yang F A and Tung C Y 1995 *Nanostruct. Mater.* **6** 977
[16] Hsu C M, Lin H M, Tsai K R and Lee P W 1994 *J. Appl. Phys.* **76** 4793
[17] Fraune M, Rüdiger U, Güntherodt G, Cardoso S and Freitas P 2000 *Appl. Phys. Lett.* **77** 3815
[18] Liu K, Nogués J, Leighton C, Masuda H, Nishio K, Roshchin I V and Schuller I K 2002 *Appl. Phys. Lett.* **81** 4434
Hoffmann A, Grimsditch M, Pearson J E, Nogués J, Macedo W A A and Schuller I K 2003 *Phys. Rev.* B **67** 220406
[19] Guo Z B, Zheng Y K, Li K B, Liu Z Y, Luo P, Shen Y T and Wu Y H 2003 *J. Appl. Phys.* **93** 7435
[20] Martín J I, Nogués J, Liu K, Vicent J L and Schuller I K 2003 *J. Magn. Magn. Mater.* **256** 449
[21] Laurent Ch, Blaszczyk Ch, Brieu M and Rousset A 1995 *Nanostruct. Mater.* **6** 317
[22] Young R A 1995 *The Rietveld Method* (Oxford: Oxford University Press) (International Union of Crystallography)
Lutterotti L and Scardi P 1990 *J. Appl. Crystallogr.* **23** 246
Lutterotti L and Gialanella S 1997 *Acta Mater.* **46** 101
[23] Joint Committee for Powder Diffraction Standards 1997 *PCPDFWIN* (Swarthmore, PA: International Center for Diffraction Data)
[24] Foner S 1963 *Phys. Rev.* **130** 183
[25] Cheng R, Borca C N, Dowben P A, Stadler S and Idzerda Y U 2001 *Appl. Phys. Lett.* **78** 521
[26] Paccard D, Schlenker C, Massenet O, Montmory R and Yelon A 1966 *Phys. Status Solidi* **16** 301
Schlenker C and Paccard D 1967 *J. Physique* **28** 611
[27] Fitzsimmons M R, Leighton C, Hoffmann A, Yashar P C, Nogués J, Liu K, Majkrzak C F, Dura J A, Fritzsche H and Schuller I K 2001 *Phys. Rev.* B **64** 104415
van Driel J, de Boer J R, Lenssen K M H and Coehoorn R 2000 *J. Appl. Phys.* **88** 975
[28] Wang J, Wang W N, Chen X, Zhao H W and Zhan W S 2000 *Appl. Phys. Lett.* **77** 2731
Tsang C and Lee K 1982 *J. Appl. Phys.* **53** 2605
[29] Miltényi P, Gierlings M, Bamming M, May U, Güntherodt G, Nogués J, Gruyters M, Leighton C and Schuller I K 1999 *Appl. Phys. Lett.* **75** 2304
[30] Binns C, Maher M J, Pankhurst Q A, Kechrakos D and Trohidou K N 2002 *Phys. Rev.* B **66** 184413
[31] Respaud M, Broto J M, Rakoto H, Fert A R, Thomas L, Barbara B, Verelst M, Snoeck E, Lecante P, Mosset A, Osuna J, Ould Ely T, Amiens C and Chaudret B 1998 *Phys. Rev.* B **57** 2925
[32] Nogués J, Morellon L, Leighton C, Ibarra M R and Schuller I K 2000 *Phys. Rev.* B **61** R6455
Ambrose T and Chien C L 1998 *J. Appl. Phys.* **83** 7222
Nogués J, Sort J, Suriñach S, Muñoz J S, Baró M D, Bobo J F, Lüder U, Haanappel E, Fitzsimmons M R, Hoffmann A and Cai J W 2003 *Appl. Phys. Lett.* **82** 3044
Camarero J, Pennec Y, Vogel J, Pizzini S, Cartier M, Fettar F, Ernult F, Tagliaferri A, Brookes N B and Dieny B 2003 *Phys. Rev.* B **67** 020413
Nogués J, Lederman D, Moran T J and Schuller I K 1996 *Phys. Rev. Lett.* **76** 4624
Leighton C, Nogués J, Jönsson-Åkerman B J and Schuller I K 2000 *Phys. Rev. Lett.* **84** 3466
[33] Georgiev D and Nietz V V 1996 *J. Magn. Magn. Mater.* **154** 119
Fiebig M, Fröhlich D and Thiele H J 1996 *Phys. Rev.* B **54** R12681
Foner S 1962 *J. Appl. Phys.* **33** 1289S
[34] Bogdanov A N and Rössler U K 2003 *Phys. Rev.* B **68** 012407
Cramer N and Camley R E 2001 *Phys. Rev.* B **63** 060404(R)
Carriço A S, Camley R E and Stamps R L 1994 *Phys. Rev.* B **50** 13453